E. Robustness of LP Results

E.1. Baseline Results

Figures E.1 and E.2 display the IRFs to an unexpected oil sanction intensity shock for the U.S. and EU economies, incorporating four lags of the endogenous variables in the LP model (3). Additionally, Figures E.3 and E.4 present the IRFs from the LP model (3) with a constant and a linear trend. The results remain robust across these alternative specifications.

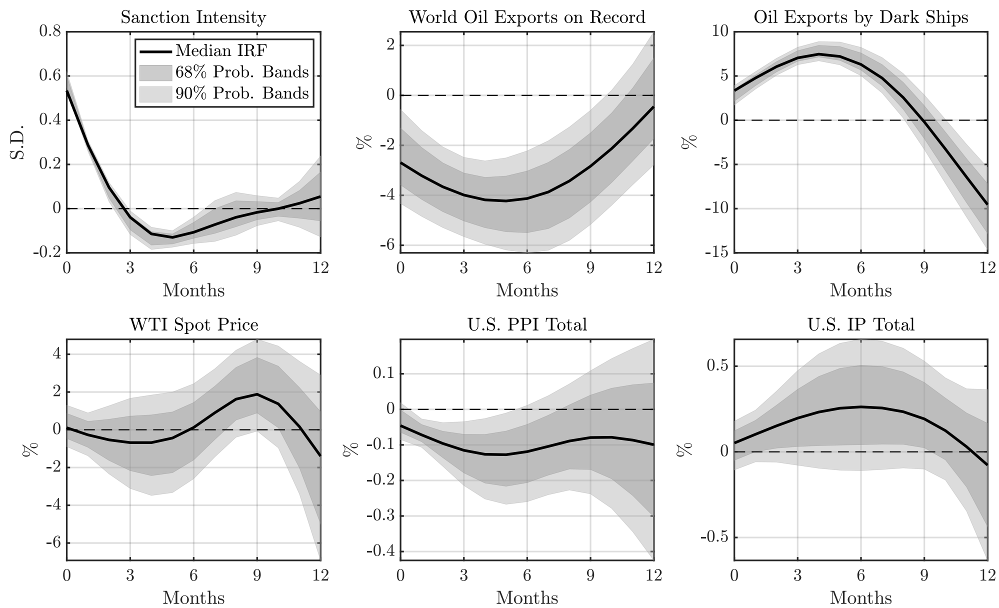

Figure E.1: IRFs to an Oil Sanction Intensity Shock for the U.S. Economy: $L = 4$

Notes. The IRFs to a one-standard-deviation unexpected oil sanction intensity shock for the U.S. economy are computed using the SLP method (Barnichon and Brownlees, 2019). Apart from incorporating four lags of the endogenous variables, the estimation follows the same specification as in Figure 12. Black solid lines represent median responses, while gray-shaded areas indicate the 68% and 90% confidence bands.

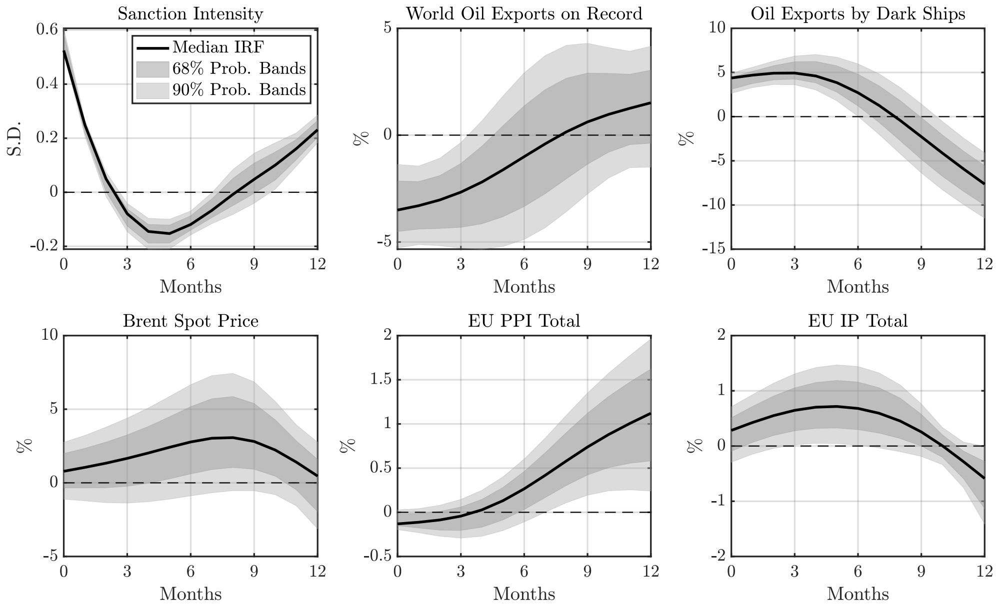

Figure E.2: IRFs to an Oil Sanction Intensity Shock for the EU Economy: $L = 4$

Notes. The IRFs to a one-standard-deviation unexpected oil sanction intensity shock for the EU economy are computed using the SLP method (Barnichon and Brownlees, 2019). Apart from incorporating four lags of the endogenous variables, the estimation follows the same specification as in Figure 13. Black solid lines represent median responses, while gray-shaded areas indicate the 68% and 90% confidence bands.

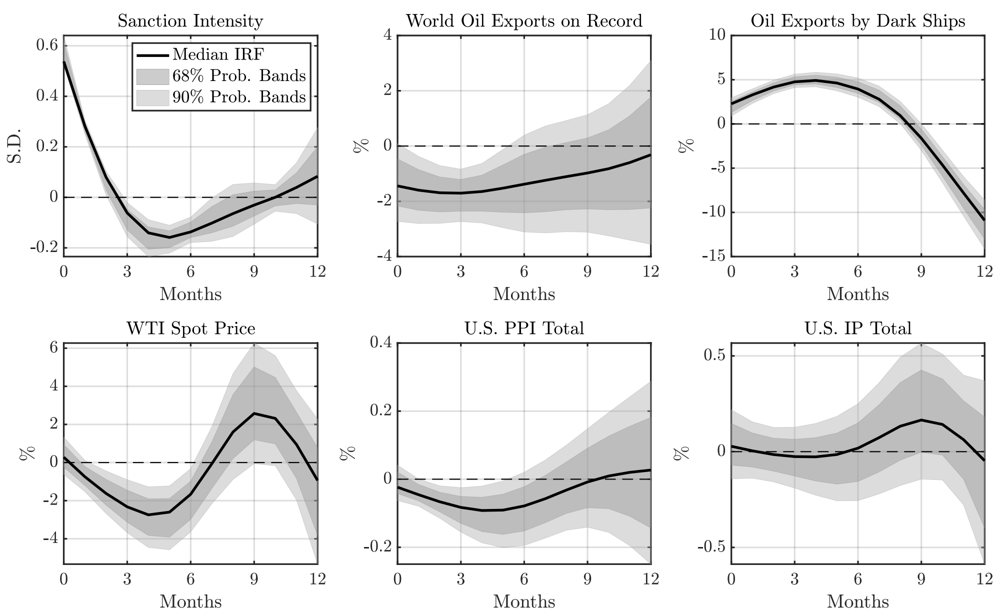

Figure E.3: IRFs to an Oil Sanction Intensity Shock for the U.S. Economy: Linear Trend

Notes. The IRFs to a one-standard-deviation unexpected oil sanction intensity shock for the U.S. economy are computed using the SLP method (Barnichon and Brownlees, 2019). Apart from incorporating both a constant and a linear trend, the estimation matches the specification used in Figure 12. Black solid lines represent median responses, while gray-shaded areas indicate the 68% and 90% confidence bands.

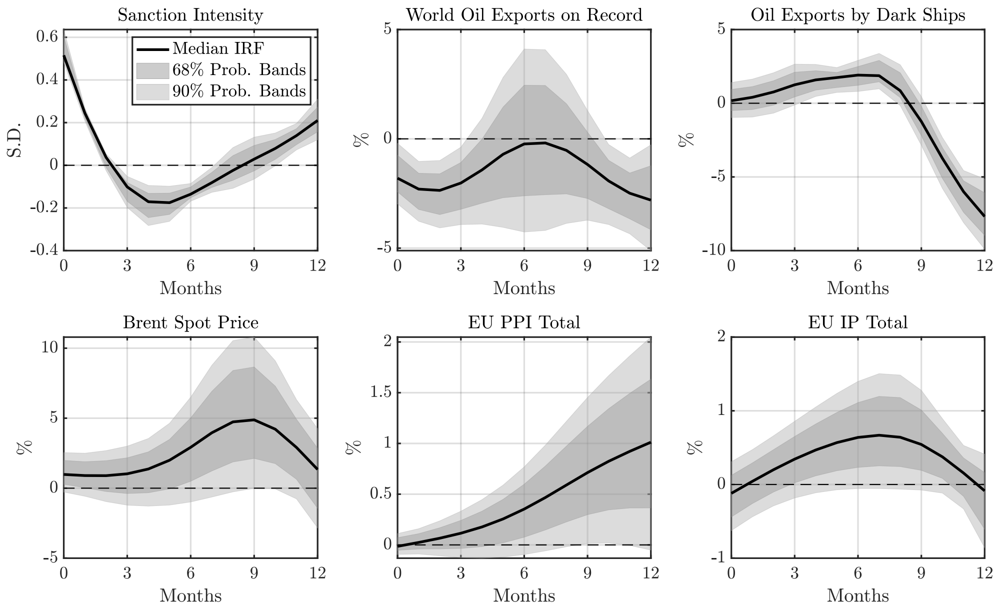

Figure E.4: IRFs to an Oil Sanction Intensity Shock for the EU Economy: Linear Trend

Notes. The IRFs to a one-standard-deviation unexpected oil sanction intensity shock for the EU economy are computed using the SLP method (Barnichon and Brownlees, 2019). Apart from incorporating both a constant and a linear trend, the estimation matches the specification used in Figure 13. Black solid lines represent median responses, while gray-shaded areas indicate the 68% and 90% confidence bands.

Figures E.5 and E.6 present the IRFs to an unexpected oil sanction intensity shock for the U.S. and EU economies, replacing the WTI spot price with the U.S. crude oil import price and the Brent spot price with the EU crude oil import price. The U.S. import price is sourced from FRED (`IR10000`), and the EU import price from Eurostat (`STS.M.I9.N.IMPR.2B0610.4.000`), both of which are manually seasonally adjusted. The results remain robust.

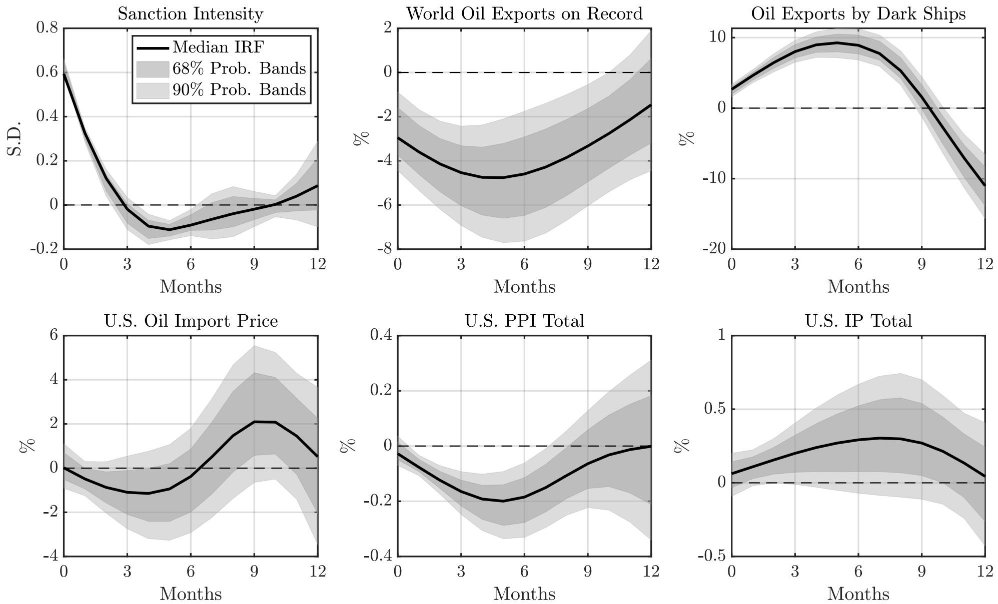

Figure E.5: IRFs to an Oil Sanction Intensity Shock for the U.S. Economy: Oil Import Price

Notes. The IRFs to a one-standard-deviation unexpected oil sanction intensity shock for the U.S. economy are computed using the SLP method (Barnichon and Brownlees, 2019). Apart from replacing the WTI spot price with the U.S. crude oil import price, the estimation specification remains identical to that used for Figure 12. Black solid lines represent median responses, while gray-shaded areas indicate the 68% and 90% confidence bands.

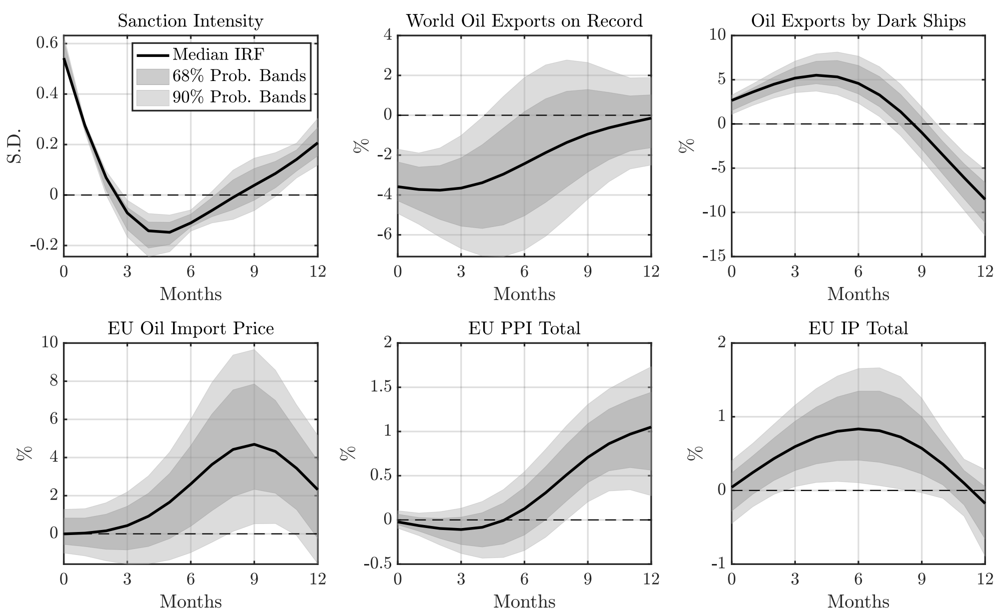

Figure E.6: IRFs to an Oil Sanction Intensity Shock for the EU Economy: Oil Import Price

Notes. The IRFs to a one-standard-deviation unexpected oil sanction intensity shock for the EU economy are computed using the SLP method (Barnichon and Brownlees, 2019). Apart from replacing the Brent spot price with the EU crude oil import price, the estimation specification remains identical to that used for Figure 13. Black solid lines represent median responses, while gray-shaded areas indicate the 68% and 90% confidence bands.

Figures E.7 and E.8 present the IRFs to an unexpected oil sanction intensity shock for the U.S. and EU economies, identified using a Cholesky-ordered SVAR model. The endogenous variables are ordered as follows: the oil sanction intensity index, recorded world seaborne crude oil exports, crude oil exports from sanctioned countries transported by dark ships, the WTI spot price, U.S./EU IP, and U.S./EU PPI.

Our timing assumption holds that an oil sanction intensity shock immediately affects all subsequent variables. Conversely, shocks to recorded world seaborne and dark-shipped oil exports influence only later variables, without affecting the sanction intensity index contemporaneously.

Overall, the IRFs are less precisely estimated for both economies. For the U.S., the median responses of the endogenous variables remain largely unchanged from Figure 12. In contrast, for the EU, the median Brent spot price response is positive for the first three months after the shock, while the total PPI response remains consistently negative across forecast horizons. However, none of these differences are statistically significant.

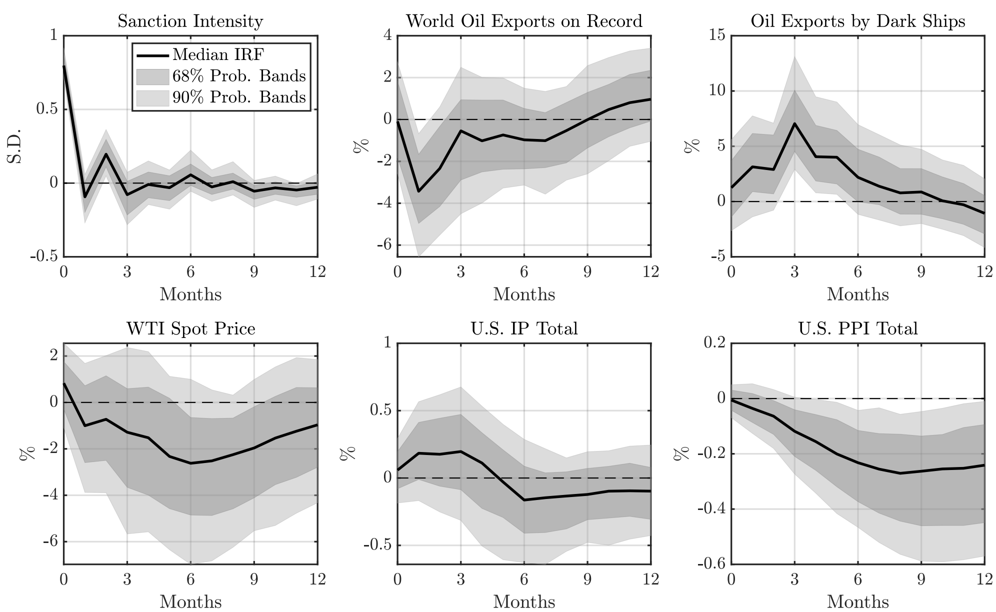

Figure E.7: IRFs to an Oil Sanction Intensity Shock for the U.S. Economy: Cholesky-Ordered SVAR

Notes. The IRFs to a one-standard-deviation unexpected oil sanction intensity shock for the U.S. economy are computed using a Cholesky-ordered SVAR model with three lags. The ordering of endogenous variables follows Figure 12, except that total PPI and IP are switched. Black solid lines represent the median responses, while the gray-shaded areas indicate the 68% and 90% confidence bands.

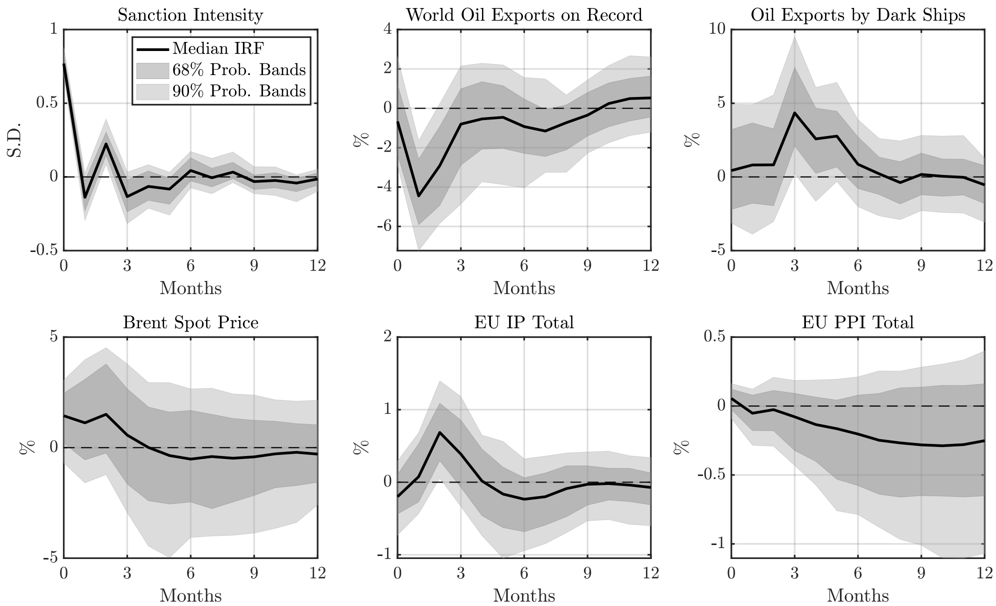

Figure E.8: IRFs to an Oil Sanction Intensity Shock for the EU Economy: Cholesky-Ordered SVAR

Notes. The IRFs to a one-standard-deviation unexpected oil sanction intensity shock for the EU economy are computed using a Cholesky-ordered SVAR model with a lag length of three. The ordering of endogenous variables mirrors that in Figure 13, except that the order of total PPI and IP is switched. Black solid lines represent median responses, while gray-shaded areas indicate the 68% and 90% confidence bands.

Figure E.9 presents the IRFs to an unexpected oil sanction intensity shock for OPEC countries. The IRFs are derived using the LP model (3), which includes the following monthly time series: (i) the sanction intensity index, (ii) crude oil exports from sanctioned countries transported by dark ships, (iii) OPEC crude oil exports, (iv) OPEC spot crude oil price, (v) OPEC net oil export revenue, and (vi) OPEC total spare crude oil production capacity. The sample spans January 2017 to December 2023.

Crude oil export data are sourced from the UN Comtrade database (HS code 2709), and spot crude oil prices are sourced from OPEC's official website. The monthly OPEC net oil export revenue series is interpolated using the Chow-Lin method (Chow and Lin, 1971), based on the annual series from the U.S. Energy Information Administration (EIA) and the monthly OPEC crude oil export value. Spare production capacity data are also obtained from the EIA.

The oil sanction intensity shock is identified by controlling for two lags of the endogenous variables, as determined by the HQIC criterion, and estimating the LP model from horizon $k = 0$. Similar to the estimation for the U.S. and EU economies, the IRFs are approximated using the SLP method described in Barnichon and Brownlees (2019).

Tracing the dynamic responses of OPEC-related variables shows that an unexpected rise in oil sanction intensity reduces OPEC's oil export volume, price, and net revenue, though to varying degrees. Meanwhile, OPEC's spare production capacity increases, indicating a less tight market for its oil. As dark-shipped oil exports decline after the sixth month, while OPEC's oil exports continue falling, OPEC's spot crude price rises significantly, boosting net oil export revenue. Spare capacity remains elevated, reflecting OPEC's strategy of using supply cuts to restore revenue margins.

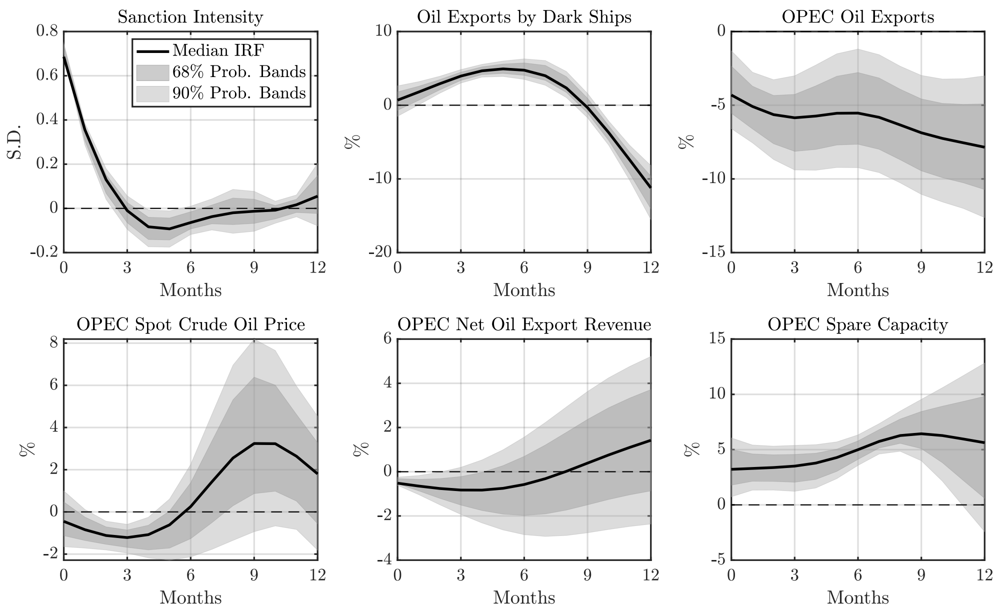

Figure E.9: IRFs to an Oil Sanction Intensity Shock for OPEC Countries

Notes. The IRFs to a one-standard-deviation unexpected oil sanction intensity shock for OPEC countries are computed using the SLP method (Barnichon and Brownlees, 2019). Black solid lines represent median responses, while gray-shaded areas indicate the 68% and 90% confidence bands.

Lastly, Figure E.10 presents the IRFs to an unexpected oil sanction intensity shock for China. The impulse responses are derived using the LP model in Equation (3), which includes the following monthly time series: (i) the sanction intensity index, (ii) crude oil exports from sanctioned countries transported by dark ships, (iii) China's PPI for mining and quarrying, (iv) China's VAI for mining, (v) China's PPI for manufactured, and (vi) China's VAI for manufacturing, covering January 2017 to December 2023. All China-related data are sourced from the National Bureau of Statistics of China.

The oil sanction intensity shock is identified by controlling for three lags of endogenous variables, as determined by the HQIC criterion, and estimating the LP model from horizon $k = 0$.

As shown in Figure E.10, China benefits from reduced costs and increased production in both the energy (proxied by mining and quarrying) and manufacturing industries.

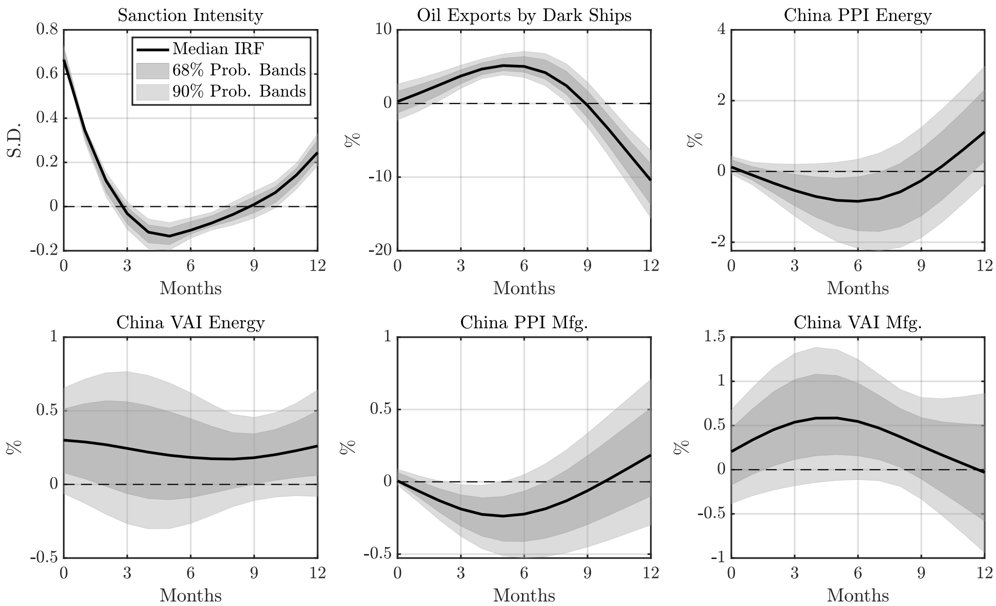

Figure E.10: IRFs to an Oil Sanction Intensity Shock for China

Notes. The IRFs to a one-standard-deviation unexpected oil sanction intensity shock for China are computed using the SLP method (Barnichon and Brownlees, 2019). Black solid lines represent median responses, while gray-shaded areas indicate the 68% and 90% confidence bands.

E.2. Propagation Channels

To complement Figures 14 and 15 in the main text, Figures E.11 and E.12 show the full IRFs to an unexpected oil sanction intensity shock for the U.S. and EU economies, respectively.

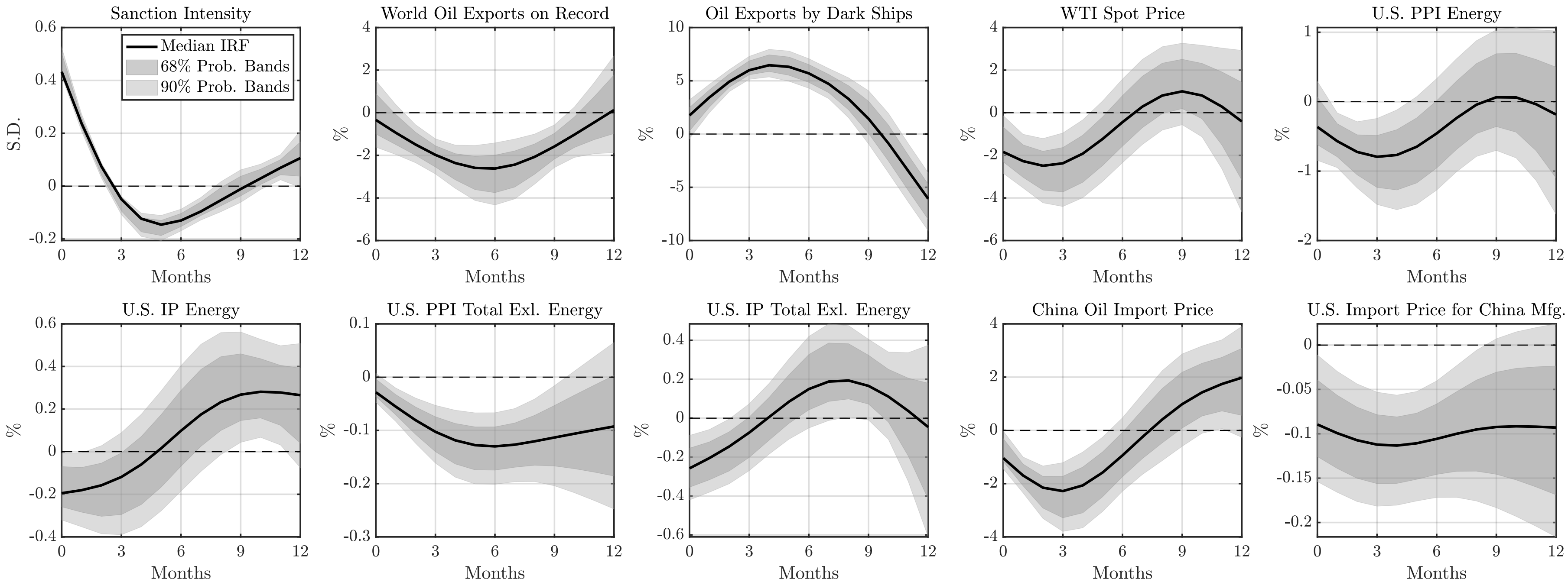

Figure E.11: IRFs to an Oil Sanction Intensity Shock for the U.S. Economy: Propagation Channels (Full IRFs)

Notes. The IRFs to a one-standard-deviation unexpected oil sanction intensity shock for the U.S. economy are computed using the SLP method described in Barnichon and Brownlees (2019). The estimation specifications follow the baseline outlined in Section 5.1 of the main text, with two modifications: (i) two additional variables – China's crude oil import price and the U.S. import price for manufacturing goods from China, averaged across NAICS sectors 31 to 33 – are included, and (ii) the total PPI and IP for the U.S. economy are replaced by the PPI and IP for the energy and non-energy sectors. Black solid lines represent median responses, while gray-shaded areas indicate the 68% and 90% confidence bands.

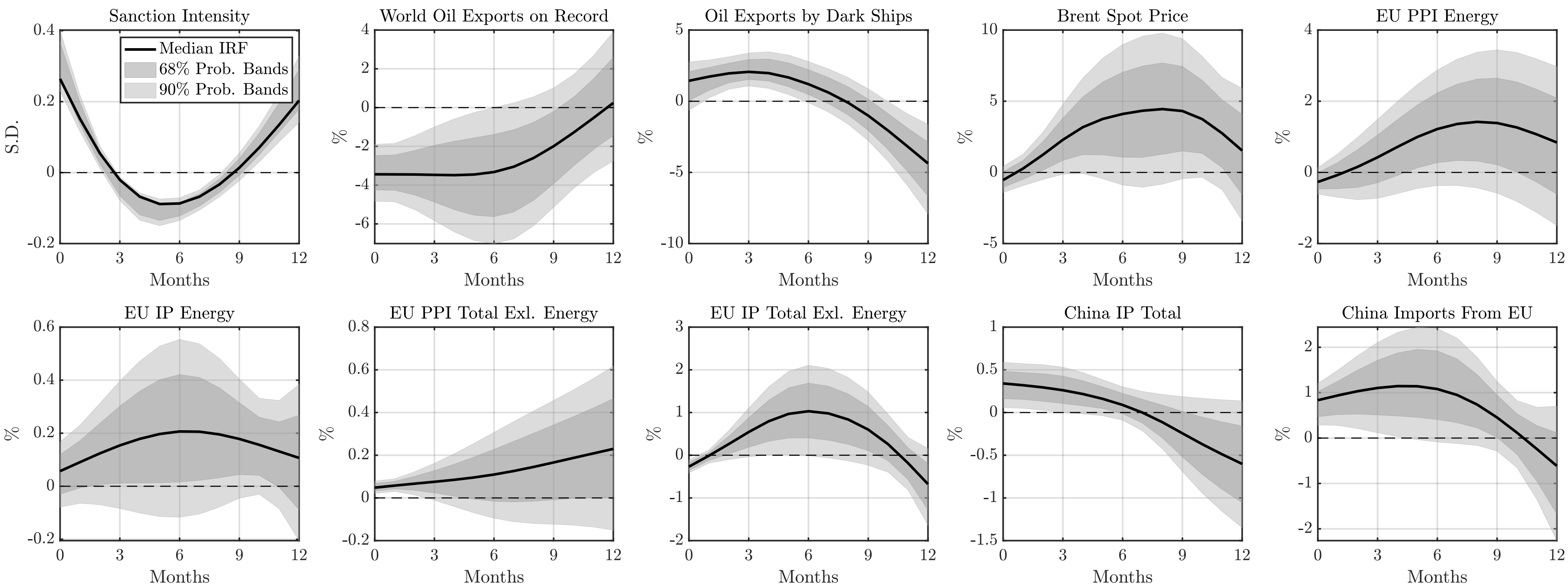

Figure E.12: IRFs to an Oil Sanction Intensity Shock for the EU Economy: Propagation Channels (Full IRFs)

Notes. The IRFs to a one-standard-deviation unexpected oil sanction intensity shock for the EU economy are computed using the SLP method described in Barnichon and Brownlees (2019). The estimation specifications follow the baseline outlined in Section 5.1 of the main text, with two modifications: (i) two additional variables – China's total IP and its total import value from the EU – are included, and (ii) the total PPI and IP for the EU economy are replaced by the PPI and IP for the energy and non-energy sectors. Black solid lines represent median responses, while gray-shaded areas indicate the 68% and 90% confidence bands.

Figure E.13 presents the IRFs to an unexpected oil sanction intensity shock for the U.S. economy, using the same model specification as Figure 14, except that China's oil import price is replaced with its total PPI. The monthly series for China's total PPI is sourced from the National Bureau of Statistics of China and has been seasonally adjusted.

The results indicate that this substitution has little impact, as China's total PPI consistently declines across all forecast horizons.

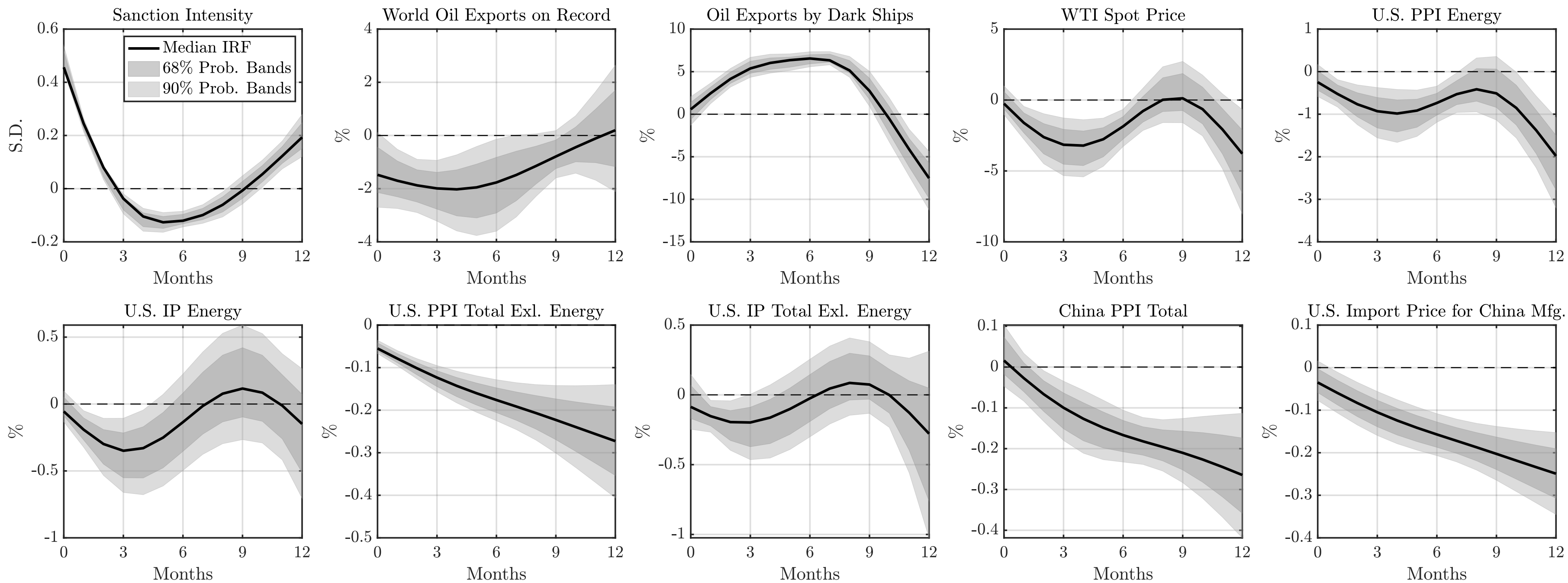

Figure E.13: IRFs to an Oil Sanction Intensity Shock for the U.S. Economy: China's Total PPI

Notes. The IRFs to a one-standard-deviation unexpected oil sanction intensity shock for the U.S. economy are computed using the same LP model specification as in Figure 14, with the exception of replacing China's oil import price with its total PPI. Black solid lines represent median responses, while gray-shaded areas indicate the 68% and 90% confidence bands.

Figure E.14 presents the IRFs to an unexpected oil sanction intensity shock for the U.S. economy, using the same model specification as Figure 14, except that the U.S. import price for China's manufactured goods is replaced with the import price for all Chinese products. The monthly series for the U.S. import price of all Chinese products is sourced directly from FRED (`CHNTOT`) and has been seasonally adjusted. Once again, the results appear largely unaffected by this variable substitution.

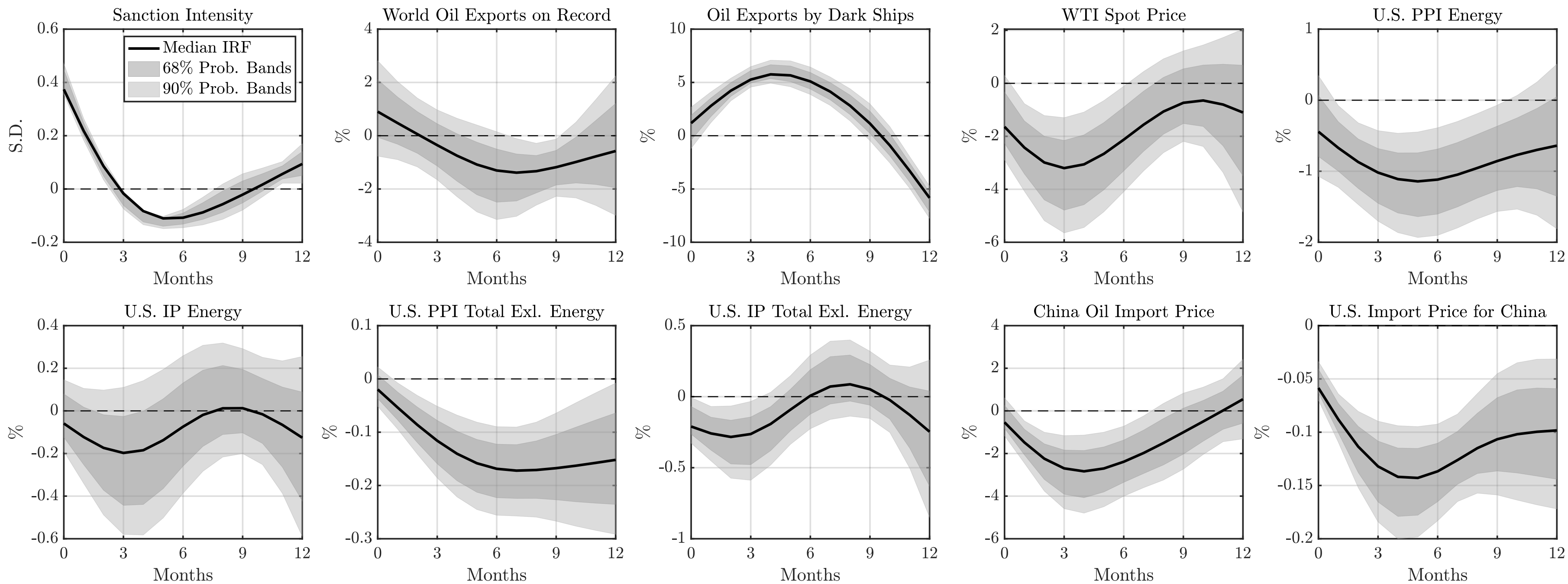

Figure E.14: IRFs to an Oil Sanction Intensity Shock for the U.S. Economy: U.S. Import Price for China

Notes. The IRFs to a one-standard-deviation unexpected oil sanction intensity shock for the U.S. economy are computed using the same LP model specification as in Figure 14, except that the U.S. import price for China's manufactured goods is replaced with the import price for all Chinese goods. Black solid lines represent median responses, while gray-shaded areas indicate the 68% and 90% confidence bands.

Figure E.15 presents the IRFs to an unexpected oil sanction intensity shock for the U.S. economy, based on an 11-variable LP model (3). This model extends the ten endogenous variables from Figure 14 by adding U.S. crude oil exports, using data from the U.S. EIA.

The ten original variables exhibit responses similar to those in Figure 14. U.S. crude oil exports closely track the WTI spot price, declining sharply in the first six months before stabilizing near the zero-response line.

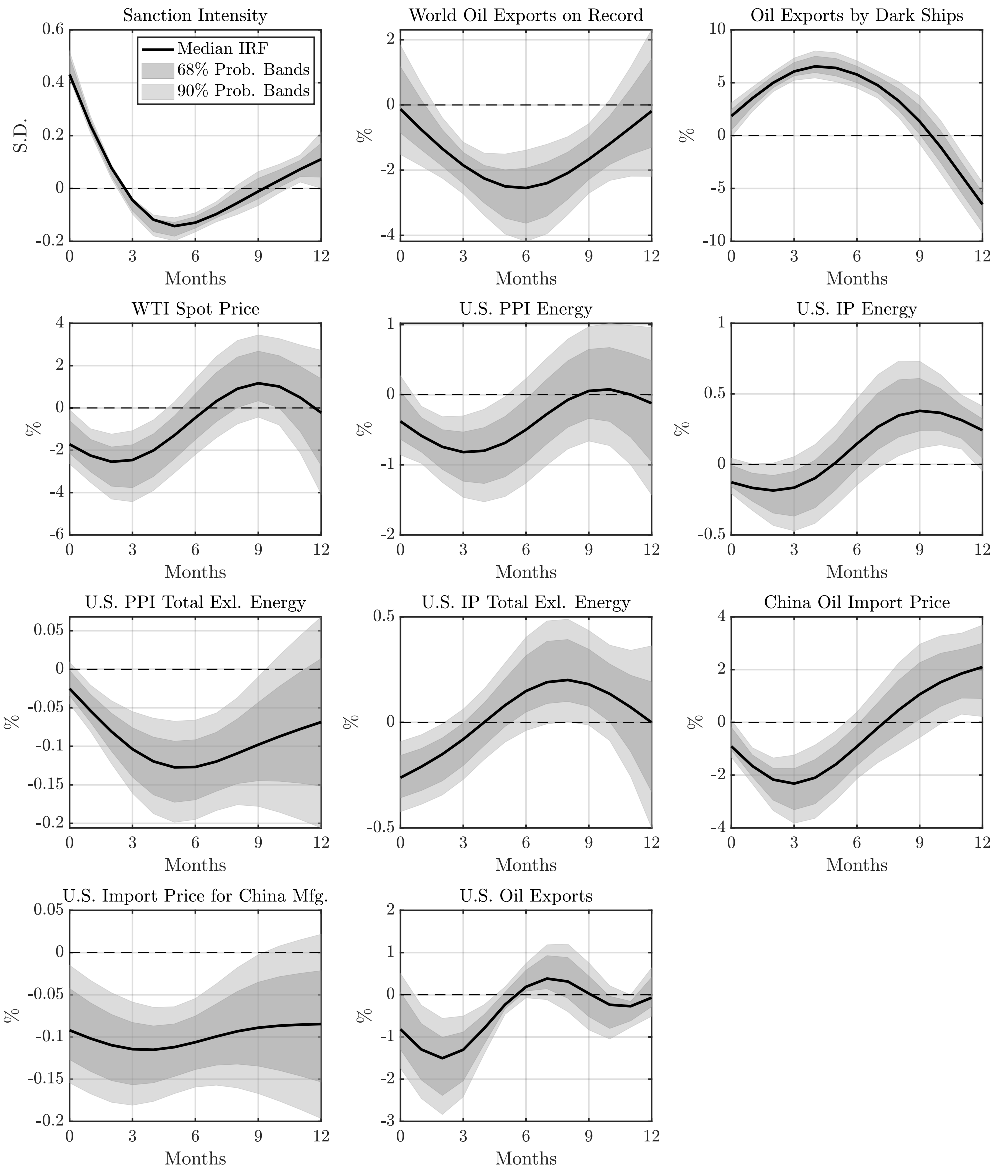

Figure E.15: IRFs to an Oil Sanction Intensity Shock for the U.S. Economy: U.S. Oil Exports

Notes. The IRFs to a one-standard-deviation unexpected oil sanction intensity shock for the U.S. economy are computed using an 11-variable LP model (3), which includes the same ten endogenous variables as in Figure 14 of the main text, plus U.S. crude oil exports. The model is estimated using the SLP method outlined in Barnichon and Brownlees (2019). Black solid lines represent median responses, while gray-shaded areas indicate the 68% and 90% confidence bands.

Figure E.16 compares the IRFs for the U.S. economy with and without two China-related variables – China's oil import price and the U.S. import price for Chinese manufactured goods. In the first three months, the median responses of U.S. energy and non-energy IP are closer to the zero-response lines than in Panels 14b and 14d of the main text. This suggests a positive omitted variable bias, where lower Chinese import prices support short-term U.S. production.

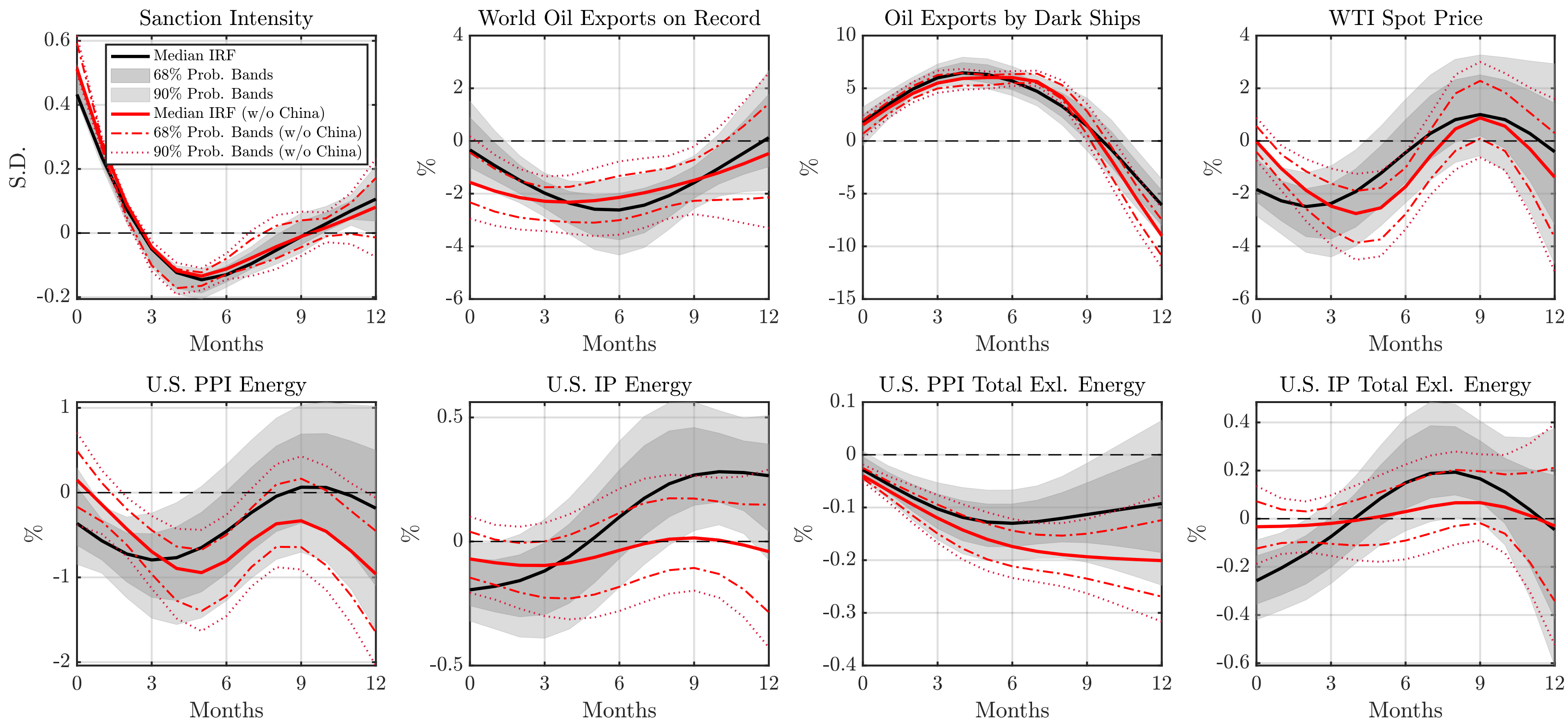

Figure E.16: IRFs to an Oil Sanction Intensity Shock for the U.S. Economy: With and Without China-Related Variables

Notes. The IRFs to a one-standard-deviation unexpected oil sanction intensity shock for the U.S. economy are computed using both a 10-variable LP model, as in Figure 14, and a counterfactual 8-variable LP model that excludes the two China-related variables: China's oil import price and the U.S. import price for China's manufactured products. The IRFs are approximated using the SLP method (Barnichon and Brownlees, 2019). The black solid lines represent the median responses estimated from the 10-variable LP model, with gray-shaded areas showing the corresponding 68% and 90% confidence bands. The red solid lines show the median responses from the counterfactual 8-variable LP model, while the red dash-dotted and dotted lines indicate the respective 68% and 90% confidence bands.

References for Appendices

Adland, R., Cariou, P., and Wolff, F.-C. (2020). Optimal Ship Speed and the Cubic Law Revisited: Empirical Evidence From an Oil Tanker Fleet. *Transportation Research Part E: Logistics and Transportation Review*, 140:101972.

Androjna, A., Pavić, I., Gucma, L., Vidmar, P., and Perkovič, M. (2024). AIS Data Manipulation in the Illicit Global Oil Trade. *Journal of Marine Science and Engineering*, 12(1).

Ballinger, O. (2024). Automatic Detection of Dark Ship-To-Ship Transfers Using Deep Learning and Satellite Imagery. *arXiv preprint*.

Barnichon, R. and Brownlees, C. (2019). Impulse Response Estimation by Smooth Local Projections. *Review of Economics and Statistics*, 101(3):522–530.

Bernabé, P., Gotlieb, A., Legeard, B., Marijan, D., Sem-Jacobsen, F. O., and Spieker, H. (2024). Detecting Intentional AIS Shutdown in Open Sea Maritime Surveillance Using Self-Supervised Deep Learning. *IEEE Transactions on Intelligent Transportation Systems*, 25(2):1166–1177.

Chow, G. C. and Lin, A. (1971). Best Linear Unbiased Interpolation, Distribution, and Extrapolation of Time Series by Related Series. *Review of Economics and Statistics*, 53:372–375.

Chupilkin, M., Javorcik, B., Peeva, A., and Plekhanov, A. (2024). Decision to Leave: Economic Sanctions and Intermediated Trade. Working paper, European Bank for Reconstruction and Development.

Li, Y., Bai, X., Wang, Q., and Ma, Z. (2022). A Big Data Approach to Cargo Type Prediction and Its Implications for Oil Trade Estimation. *Transportation Research Part E: Logistics and Transportation Review*, 165:102831.

Lloyd, S. (1982). Least Squares Quantization in PCM. *IEEE Transactions on Information Theory*, 28(2):129–137.

Lloyd's List Intelligence (2023). Shifty Shades of Grey: The Different Risk Profiles of the Dark Fleet Explained. Technical report, Lloyd's List Intelligence.

Lloyd's List Intelligence (2024a). Understanding AIS Spoofing: The Case of the Blazers. Seasearcher Advanced Risk & Compliance.

Lloyd's List Intelligence (2024b). Understanding AIS Spoofing: The Case of the Shanaye Queen. Seasearcher Advanced Risk & Compliance.

MacQueen, J. B. (1967). Some Methods for Classification and Analysis of Multivariate Observations. In Cam, L. M. L. and Neyman, J., editors, *Proceedings of the Fifth Berkeley Symposium on Mathematical Statistics and Probability*, volume 1, pages 281–297, Berkeley, CA. University of California Press.

Miller, G. (2023). Welcome to the Dark Side: The Rise of Tanker Shipping's 'Shadow Fleet'. FreightWaves.

Paris MoU (2018). Explanatory Note – “White,” “Grey” and “Black List”. Technical report, Paris Memorandum of Understanding on Port State Control.

Ristic, B., La Scala, B., Morelande, M. R., and Gordon, N. (2008). Statistical Analysis of Motion Patterns in AIS Data: Anomaly Detection and Motion Prediction. In *2008 11th International Conference on Information Fusion*, pages 1–7, Cologne, Germany.

Rodger, M. and Guida, R. (2022). Mapping Dark Shipping Zones Using Multi-Temporal SAR and AIS Data for Maritime Domain Awareness. In *2022 IEEE International Geoscience and Remote Sensing Symposium*, pages 3672–3675, Kuala Lumpur, Malaysia.

Rong, H., Teixeira, A., and Guedes Soares, C. (2024). A Framework for Ship Abnormal Behaviour Detection and Classification Using AIS Data. *Reliability Engineering & System Safety*, 247:110105.

Triebert, C., Migliozzi, B., Cardia, A., Xiao, M., and Botti, D. (2023). Fake Signals and American Insurance: How a Dark Fleet Moves Russian Oil. The New York Times.

U.S. Department of State (2020). Sanctions advisory for the maritime industry, energy and metals sectors, and related communities. Technical report, U.S. Department of State, U.S. Department of the Treasury’s Office of Foreign Assets Control, and U.S. Coast Guard.

Yan, Z., Xiao, Y., Cheng, L., Chen, S., Zhou, X., Ruan, X., Li, M., He, R., and Ran, B. (2020). Analysis of Global Marine Oil Trade Based on Automatic Identification System (AIS) Data. *Journal of Transport Geography*, 83:102637.